International Journal of Mass Spectrometry 283 (2009) 77–84

Contents lists available at ScienceDirect

International Journal of Mass Spectrometry

journal homepage: www.elsevier.com/locate/ijms

Gas-phase infrared spectroscopy of the protonated dipeptides H^+PheAla and H^+AlaPhe compared to condensed-phase results

Robert C. Dunbar[a,*], Jeffrey D. Steill[b], Nick C. Polfer[b,c], Jos Oomens[b]

[a] Department of Chemistry, Case Western Reserve University, 10900 Euclid Avenue, Cleveland, OH 44106, United States
[b] FOM Institute for Plasma Physics "Rijnhuizen", Edisonbaan 14, 3439MN Nieuwegein, The Netherlands
[c] Department of Chemistry, University of Florida, Gainesville, FL 32611, United States

ARTICLE INFO

Article history:
Received 20 November 2008
Received in revised form 2 February 2009
Accepted 4 February 2009
Available online 12 February 2009

Dedicated to Mike Bowers on his 70th birthday in recognition of his friendship, service and notable contributions to science.

Keywords:
IRMPD
Protonated dipeptide
Gas-phase ion
IR spectroscopy
Free electron laser

ABSTRACT

The influence of the physical environment on the structures of biomolecules is considered here for the dipeptide model H^+AlaPhe cation, by making use of infrared multiple-photon dissociation (IRMPD) spectroscopy complemented by DFT calculations. The gas-phase structures of this peptide are also compared to the related peptide cations H^+PheAla and H^+AlaAla. The gas-phase IRMPD spectra of the Phe-containing cations are compared to previous studies, including the X-ray-crystallographic crystal structure for the H^+AlaPheCl$^-\cdot 2H_2O$ salt, a recent IRMPD spectrum of H^+AlaAla, and a recent determination of the IR absorption spectrum of the H^+AlaPheCl$^-$ salt in a liquid-crystal host matrix, as well as recent cryogenic ion trap results for H^+TyrAla and H^+AlaTyr. Between the gas-phase H^+AlaPhe ion and the H^+AlaPheCl$^-\cdot 2H_2O$ crystal a conformational switch is observed, induced by hydrogen bonding with a water of crystallization, involving a 180° rotation of the COOH group. The hoped-for comparison of the gas-phase IR spectra with the liquid-crystal matrix IR spectrum was frustrated, because the literature matrix spectrum seems most likely to be that of a protonated homodimer of the dipeptide rather than the protonated monomer. The IRMPD spectra of H^+AlaPhe and H^+PheAla are very similar, with only minor peak shifts suggesting small differences in local interactions within a similar overall architecture. The H^+AlaAla spectrum was also similar, and no significant reorganization of the structure seems to result from the presence or position of the aromatic ring. The spectra give highly satisfactory matches to the predicted IR spectra computed for the most stable conformers of the protonated dipeptides. It is suggested that the NH_3^+ proton is shared through hydrogen bonding to the amide C═O, giving a distinctive broadening of the associated H-bending mode.

1. Introduction

Recent advances in laser technology have made possible the exploration of the gas-phase infrared spectroscopy of a variety of ionic species, including the use of sources based on non-linear frequency down-conversion in the 2000–4000 cm^{-1} region, and the use of free electron lasers usually between 400 and 2500 cm^{-1}. Much attention has been given to protonated and metal-cationized amino acids and related species, and larger ions, such as dipeptides and small oligopeptides, are now being increasingly addressed [1–7]. Complementary data from different techniques happen to be available for one particular protonated dipeptide, H^+AlaPhe, that makes it a particularly interesting target for expanding our understanding of the effect of the physical environment on structure. Several studies have been published on this cation, including an X-ray crystallographic structure of the H^+AlaPheCl$^-\cdot 2H_2O$ salt [8], a solid matrix IR spectrum of the HCl·AlaPhe complex [9], a gas-phase free electron laser infrared multiple-photon dissociation (FEL IRMPD) spectrum of the aliphatic analog H^+AlaAla [1], and gas-phase FEL IRMPD spectra of alkali-cationized PheAla and AlaPhe [10]. (All except the first of these publications are accompanied by *ab initio* and/or DFT calculations.) This wealth of data gives an exceptionally broad context for consideration and interpretation of the gas-phase IRMPD spectroscopy of the H^+AlaPhe ion, which we present here along with its sequence-reversed analogue H^+PheAla. A further useful point of comparison is the recent study of H^+AlaTyr and H^+TyrAla, denoted here as H^+[Ala,Tyr], which used ultraviolet spectroscopy and IRMPD in the hydrogen-stretching region to establish conformations at 6 K [11].

Several noteworthy points are addressed within this context, based on our IRMPD spectra. (1) We can ask whether the position of the aromatic residue (PheAla vs. AlaPhe) has any observable consequences for the IR spectroscopy or for the architecture of the

* Corresponding author. Tel.: +1 216 368 3712; fax: +1 216 368 3006.
E-mail addresses: rcd@po.cwru.edu (R.C. Dunbar), J.D.Steill@Rijnhuizen.nl (J.D. Steill), polfer@chem.ufl.edu (N.C. Polfer), J.Oomens@rijnhuizen.nl (J. Oomens).

1387-3806/$ – see front matter © 2009 Elsevier B.V. All rights reserved.
doi:10.1016/j.ijms.2009.02.001

Table 1
Calculated relative thermochemistry of various low-energy conformations of the protonated dipeptides (B3LYP/6-31+G(d,p), kJ mol^{-1}, ΔG at 298 K). The columns labeled "Ref. [11]" give the structure labels of those conformers of H$^+$AlaTyr and H$^+$TyrAla calculated in Ref. [11] that correspond to structures calculated in the present study.

H$^+$AlaPhe				H$^+$PheAla			
	Ref. [11]	ΔH	ΔG		Ref. [11]	ΔH	ΔG
TransA1	III	0	1	TransA1	I (A)[a]	0	0
TransA1′	I	0	0	TransA1′	I (G)[a]	4	5
TransA1″		7	6	TransA1″		13	13
TransA2	II	0	1	TransA2	II	5	4
TransA2′	IV	3	1	TransA2′		7	8
TransO1		1	3	TransA2″	III	12	13
TransO1′		3	4	TransO1		13	14
TransO1″		8	9	TransA1R		16	14
TransA2R		9	5	TransO2″R		26	27
TransA1′R		13	10	TransA2″R		26	24
TransA1″R		22	19	TransO1R		35	32
TransO2R		12	14	CisA3		21	24
TransO1′R		15	17	CisA3R		82	82
TransO1″R		26	28				
CisA3		14	15				

[a] The (A) and (G) designations denote respectively the *anti* and *gauche* orientations of the corresponding H$^+$TyrAla structures described in Ref. [11].

most stable conformation of the protonated ion. (2) We can see whether the presence of the aromatic residue has any consequences in comparison with the aliphatic H$^+$AlaAla, whose IRMPD spectrum and most stable conformation have been reported by Lucas et al. [1]. (3) This spectrum may offer a first opportunity for the direct comparison of the IR spectroscopy of a protonated dipeptide in the gas phase versus the non-aqueous condensed phase, since a spectrum was recently reported [9] that was believed to be that of H$^+$AlaPhe·Cl$^-$ in a solid matrix. (4) We can look at the effect of crystal-packing and included-water interactions on the cation structure, taking advantage of the X-ray crystallographic structure of H$^+$AlaPheCl$^-$·2H$_2$O determined by Cortrait and Barrans [8]. (5) The IRMPD spectra are sufficiently well resolved to allow us to point out the likely presence of a mobile proton in the ions whose presence apparently correlates with a characteristic peak broadening of the associated H-bending mode.

2. Experimental and computational

2.1. Mass spectrometry and infrared spectroscopy

IRMPD spectra have been obtained using the free electron laser FELIX coupled to a home-built Fourier transform ion cyclotron resonance (FTICR) mass spectrometer described in detail elsewhere [12,13]. Briefly, protonated dipeptides are generated by electrospray ionization (ESI) using a commercial Z-Spray source (Micromass, Manchester, UK). Ions are accumulated in a linear hexapole rf trap and pulse injected into the ICR cell via a 1-m long rf octopole ion guide. In the ICR cell, the ions are mass-selectively isolated using a SWIFT pulse and subsequently irradiated with 10–20 macro-pulses from FELIX. A 5-μs macro-pulse consists of a train of ∼1-ps micropulses spaced by 1 ns and has a pulse-energy of about 35 mJ. For this experiment, the laser frequency was tuned between 600 (or 900) and 1900 cm^{-1}. After the irradiation, the intensities of the remaining parent ions and of the IR-induced fragment ions are determined by a standard excite/detect sequence and the yield is calculated as the summed fragment intensities divided by the total ion intensity (i.e., parent plus fragments). The fragment yield is normalized for laser intensity, and then plotted versus the laser wavelength to produce an IRMPD spectrum.

Dipeptide samples were obtained from Sigma–Aldrich (St. Louis, MO) and dissolved in a 70/30 methanol/water mixture. Under our irradiation conditions, the protonated dipeptide (m/z 237) is observed to fragment mainly into m/z 166, which results from cleavage of the amide bond giving a protonated phenylalanine as fragment.

2.2. Computational protocol

The conformation space of the two H$^+$[Ala,Phe] species was initially searched using Hyperchem 7.5. Usage-directed searching of torsional angles was used, with variation of all backbone torsions plus the hydroxyl torsion. No computational level more economical than Hartree-Fock was found adequate to treat the interactions of the phenyl ring, so initial searches were made at the HF STO-3G level, inspecting about 400 trial structures for H$^+$AlaPhe and 200 for H$^+$PheAla. In addition the structural families found by Lucas et al. [1] in their comprehensive search of H$^+$AlaAla were drawn on as the basis for generating additional candidate structures. A set of structures with preliminary low-level energies within 20 kcal mol^{-1} of the most stable were fully optimized at the DFT B3LYP/6-31+g(d,p) level as displayed in Table 1, and vibrational spectra were calculated for the low-energy conformers. A scaling factor of 0.975 for the IR frequencies was used, which has been found satisfactory for IRMPD spectra of the mid-IR spectra of various similar systems at this computational level [10,14]. Free energies were calculated using rigid-rotor harmonic-oscillator entropies. As Table 1 shows, the free energy corrections did not result in many significant changes in the relative energies of the conformers.

Several apparent clerical errors in the coordinate list for the X-ray structure of H$^+$AlaPheCl$^-$·2H$_2$O (Table 2 of Ref. [8]) were corrected: evident sign errors for C8 and H26 and nonsensical values for H25 were corrected with values giving a sensible structure.

2.3. Conformations and labelling

Three torsional angle parameters can be varied to produce conformational variations of reasonable stability for H$^+$AlaPhe: these are the orientation of the COOH group around the C–C bond (angle ψ_2 of Refs. [1,15]); the rotation around the skeletal N–C bond (angle ϕ of Ref. [1]); and the orientation of the side chain of the Phe residue. The conformational searches yielded structural motifs for the most stable conformations similar to those found by Lucas et al. [1] for H$^+$AlaAla and by Paisz et al. [15] for H$^+$GlyGly. Accordingly, we have used the same labeling conventions as they assigned. Within these structural motifs, the presence of the Phe side chain introduces three conformational variations with comparable energies, corresponding to different orientations of the side chain. We have distinguished these by appending primes and double primes

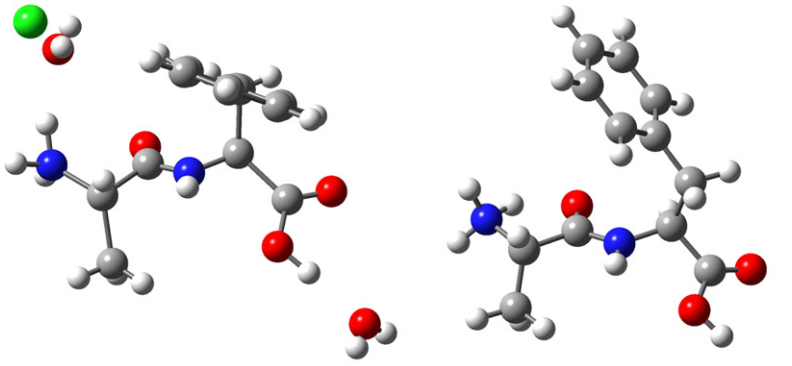

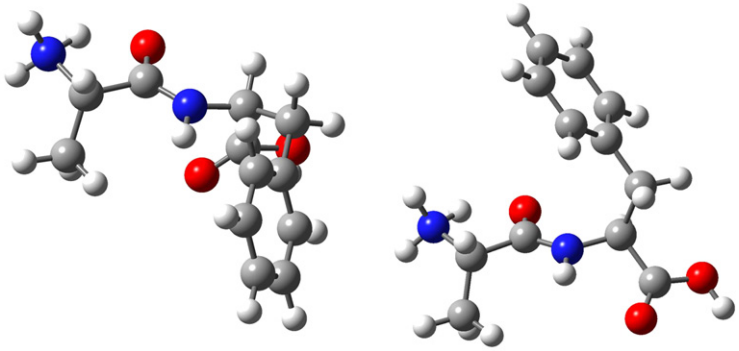

to the labels of rotational conformers. Also, as noted below, a suffix "R" has been attached to the structure designations to indicate a rotated COOH orientation.

3. Results and discussion

3.1. H^+AlaPhe structures

Several conformations of the H^+AlaPhe ion have particular interest in the later discussion, and are shown in Scheme 1. The structures illustrated in Scheme 1 include the X-ray diffraction structure of $H^+AlaPheCl^-\cdot(H_2O)_2$ [8] (**I**), the computed minimized structure of H^+AlaPhe of Koleva et al. [9] (**II**), the most stable side chain rotational conformer of the TransA2 isomer of H^+AlaPhe (**III**), and the most stable side chain rotational conformer of the TransA1 isomer (**IV**) determined in the present study.

Structures for a number of other conformations of H^+AlaPhe as well as H^+PheAla are displayed in the Supplementary Material.

The most stable calculated structure reported by Lucas et al. [1] for H^+AlaAla was TransA1, which was also the most stable structure we found for H^+AlaPhe (Scheme 1, **IV**). Given these values of ψ_2 and ϕ, two orientations of the side chain gave very similar energies, and these are designated here respectively as unprimed and singly primed labels, TransA1 and TransA1′. Structure **IV** of Scheme 1 shows the second of these, while structure **I** of Scheme 1, although it differs from the TransA1 motif, can be referred to as illustrating the unprimed side chain orientation. The third possible orientation of the Phe side chain is designated with a double prime, and was found consistently to give structures less stable by amounts on the order of 10 kJ mol^{-1} compared to the unprimed and singly primed structures.

As will be laid out below, the X-ray structure of the crystalline complex differs from these most stable gas-phase structures in that the carboxyl group is reoriented (i.e., the angle ψ_2 is 180° rotated), as shown in Scheme 1, **I**. Here we will use the shorthand "R" to designate the class of conformations having this carboxyl orientation. Thus, the X-ray structure **I** can be designated systematically as TransA1R. Note that the amide H is hydrogen bonded to the C=O in the TransA1 class of conformations, while it is hydrogen bonded to the OH group in the TransA1R class.

The structure that was optimized and reported by Koleva et al. [9] is similar to the X-ray structure, but differs in the side chain orientation. It is shown as **II** in Scheme 1, and has the systematic designation TransA1′R. As discussed below, we do not believe that this species was actually the species observed in their IR spectra.

Lucas et al. [1] found another class of low-energy structures, TransA2, differing from TransA1 in having a different ϕ value. This will be seen to be a very favorable conformation for H^+AlaPhe, and is shown as **III** in Scheme 1. Lucas et al. [1] also found a favorable *cis* conformation for H^+AlaAla, which they designated CisA3, but we found the *cis* skeletal conformation to be less favorable for H^+AlaPhe.

Finally, an interesting possibility for all the dipeptides in the TransA1 and TransA2 geometries (among others) is transfer of the proton from the NH_3^+ group to the amide C=O to which it is hydrogen bonded. This transfer often gives a distinct new local minimum on the potential energy surface, and requires only a short move of the proton with a barrier typically below the zero-point energy of the corresponding mode. The possibility that this double-well situation represents an observable shared proton is mentioned below. Following Refs. [1,15] these proton-transferred classes of conformations are designated with "O", as in TransO1′ for example.

3.2. Thermochemistry

The relative energies and free energies of the calculated conformations of both H^+AlaPhe and H^+PheAla are given in Table 1.

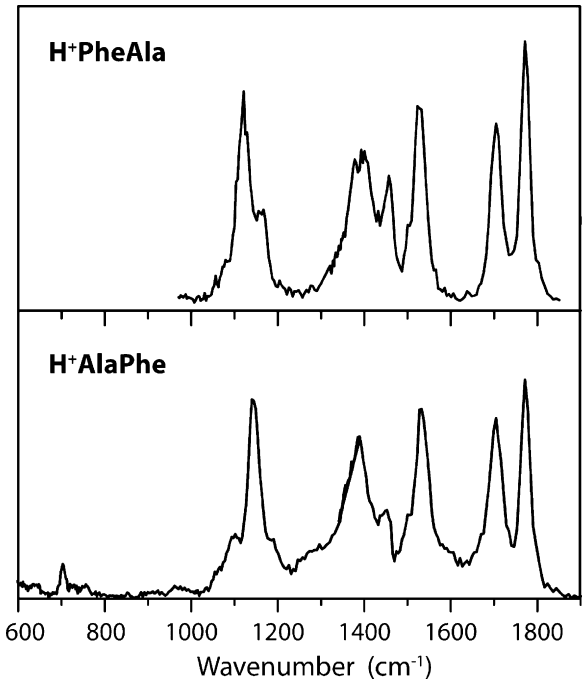

Fig. 1. IRMPD spectra of the two protonated dipeptide isomers, showing the effect of reversing the sequence of residues.

For H^+AlaPhe, a number of conformations is seen to be thermally accessible at room temperature (that is, lying within about 5 kJ mol^{-1} of the most stable one). There is very little difference in the energies of the TransA1 and TransA2 classes of conformations, representing rotation around angle ϕ. Indeed, within the "R" variants, we did not even find double potential energy wells with respect to this angle, and distinct A1 and A2 variants were not differentiated within this R class. The proton transfer represented by the A-to-O transition yielded two separate potential energy wells, separated by a barrier of around 8 kJ mol^{-1}. The mobility of this proton is discussed further below. The unprimed and primed orientations of the Phe side chain are not very different in energy, but the double-primed orientation is distinctly less favorable.

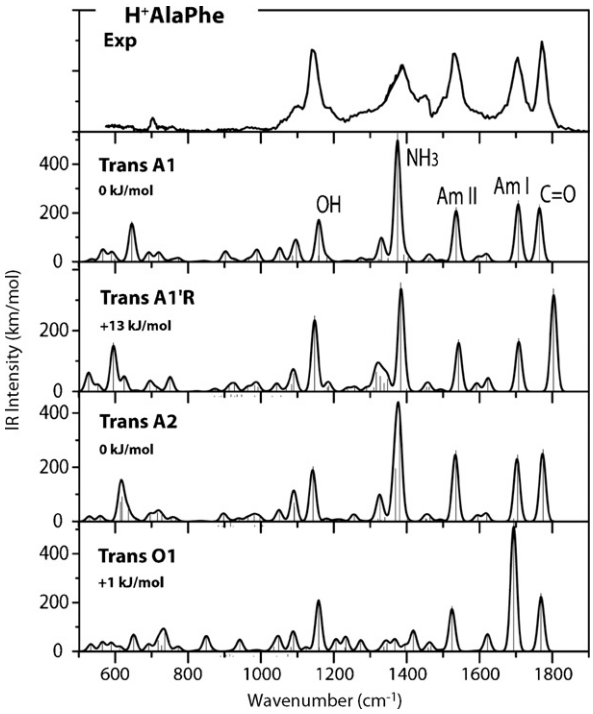

Fig. 2. Comparison of the IRMPD spectrum of H^+AlaPhe with computed spectra of several conformers. (Comparisons with other candidate structures are shown in the Supplementary Material.)

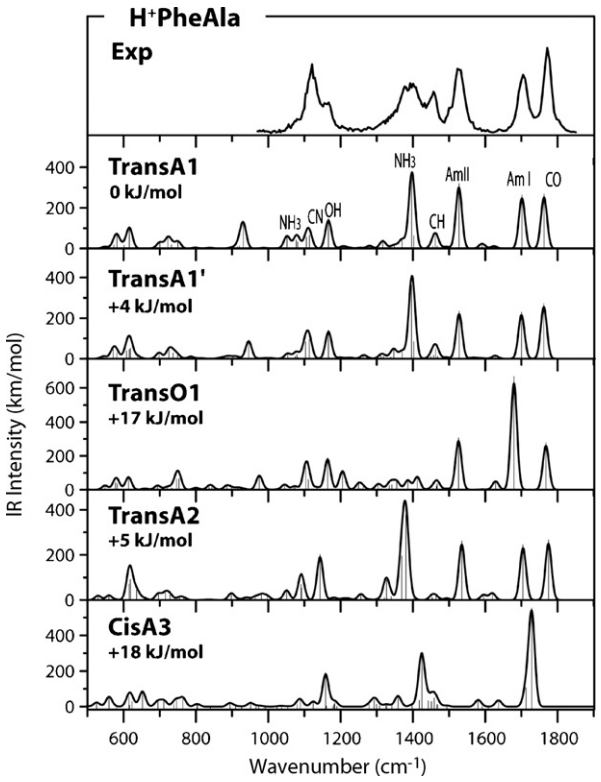

Fig. 3. Comparison of the H^+PheAla spectrum with calculated spectra of several low-energy conformers.

For H^+PheAla, the TransA1 conformation emerged as the most stable conformation by a substantial margin, and hence, based on these calculations, one would expect that this single conformation would dominate the room temperature equilibrium population. However, realistically the uncertainty in calculated relative energies is certainly not less than several kJ mol^{-1}, so that such a prediction should be taken with caution. It appears that the proton transfer to the "O" conformations is substantially uphill for H^+PheAla, in contrast to H^+AlaPhe where it is nearly thermoneutral.

3.3. IRMPD spectra, comparison of the two dipeptides and the possible effect of residue sequence

The spectra of the two protonated dipeptides are juxtaposed in Fig. 1, and are clearly very similar. If there are sequence-dependent effects, they are not revealed by the present spectra. (However, as discussed at the end of this section, the mid-IR spectral region viewed here is not very sensitive to some features of hydrogen bonding architecture, which might be more clearly revealed in the hydrogen-stretching region between 2500 and 3800 cm^{-1}.) In Figs. 2 and 3, the spectra are compared with calculations of some of the most interesting candidate conformations. As a guide to discussion, Fig. 2 notes the mode characters of the prominent vibrational features for the TransA1 conformation.

The spectra of the two ions have in common a strong peak near 1150 cm^{-1}. In the case of H^+AlaPhe, this band is unambiguously assigned as the COH bending vibration, as previously observed in the IRMPD spectra of other protonated dipeptides and metalated mono- and dipeptides [3,4], as well as in the IR absorption spectra

of neutral gas-phase amino acids. Although the calculations predict this peak reasonably well, the IRMPD intensity of this band appears to be underestimated. This intensity is also apparently underestimated in the calculations of H^+AlaAla, etc. [3] where the assigned conformation also includes a similar free carboxyl OH in-plane bend. We are less certain about the interpretation of the corresponding band for H^+PheAla. The strongest peak is at about 1115 cm^{-1}, which may be the same mode (strongly red-shifted) as that seen at 1150 cm^{-1} in H^+AlaPhe, or, more likely, one of the two modes (NH_3^+ bend and C–N stretch) predicted in this region by the calculations. It appears that the harmonic DFT calculations have some difficulty reproducing the positions and/or intensities of the modes in this region for all these dipeptides.

Many features of the spectra can be correlated with simpler known systems. The gas-phase spectra of neutral amino acids reported by Linder et al. [16] show two prominent peaks common to all the spectra for the –COOH group (C=O stretch at 1775–1780 cm^{-1}, OH in-plane bending 1110–1113 cm^{-1}), and one somewhat less intense feature that is at least partly attributed to hydrogen bending modes in the amino acid skeleton (1362–1368 cm^{-1}, CH/NH bend). The C=O stretch appears similar in our dipeptide spectra, and the OH bend is comparable, but blue-shifted in the protonated dipeptides. However, the 1300–1400 cm^{-1} region seems to provide no useful correlation between neutral amino acids and the present protonated dipeptides, which are dominated in this region by the NH_3^+ group. The other strong features in the present spectra are the Amide I and Amide II bands, which are obviously not present in the amino acid spectra of Linder et al.

The question often comes up whether a different spectral region, in particular the hydrogen-stretching region in the vicinity of 3000 cm^{-1}, would be more informative with respect to conformational and structural differences than the mid-IR region currently spanned by most free electron laser studies. While this question was not studied in detail here, two examples of computational expectations for the present systems over a wider wavelength range are shown as figures in the Supplementary Materials. Fig. S9 displays the same four candidate structures for H^+AlaPhe that were considered in Fig. 2. It can be seen that there are no dramatically better distinctions of the similar conformations to be drawn from the additional wavelengths. However, a better differentiation of TransA1 and TransA2 might be possible, based on the shift of the small peak for the NH_2–H^+ stretch from 3454 to 3509 cm^{-1}. Moreover, the distinction of TransA1′R (the X-ray structure) from the other TransA family members could be strengthened by observing the shift of the strong amide N–H stretch from about 2690 to 2732 cm^{-1}. The interesting TransO1 conformation is actually not well identified by short-wavelength features, and is much better characterized by the mid-IR wavelengths as shown in Fig. 2. The short-wavelength extension of the spectrum thus does not appear to be much more useful than the mid-IR spectrum in differentiating the various conformations of H^+AlaPhe.

Fig. S10 compares the TransA1 conformations of H^+AlaPhe and H^+PheAla. While the mid-IR spectra are very similar, as seen above in Fig. 1, it is found that the hydrogen-stretching spectral regions are very different. In particular, the hydrogen-stretching modes involving the NH_3^+ group show large sequence-dependent frequency differences. Apparently these effects are related to subtle differences in the hydrogen bonding interaction of NH_3^+ with the amide C=O group. A red shift and broadening (of the order of 20 cm^{-1} peak widths) of the hydrogen-stretching peak of strongly H-bonded protons is a recognized characteristic of such bonding (see, for instance, Refs. [17,18]). This is an interesting topic for future work on these systems. It looks as though recording the spectra of these ions at shorter wavelengths would be an incisive way to probe the effect of the sequence order on the vibrational properties, and the spectroscopy in this region will be interesting to explore further in conjunction with the observation of the H-bending peaks near 1400 cm^{-1}.

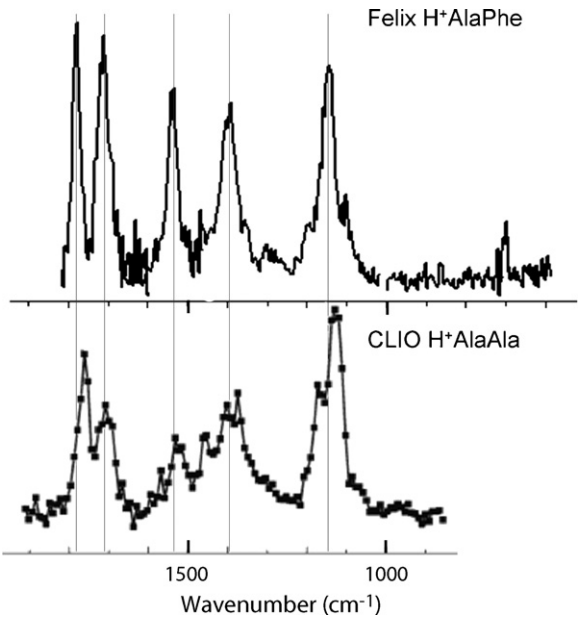

Fig. 4. Comparison of IRMPD spectra of H^+AlaPhe (present results) with H^+AlaAla (Ref. [1]).

3.4. The possible effect of the aromatic Phe residue and comparison with H^+AlaAla

The present spectra of H^+AlaPhe and H^+PheAla are very similar to the IRMPD spectrum of H^+AlaAla [1], as displayed in Fig. 4, in terms of the band positions. The five major peaks in the present H^+AlaPhe spectrum between 900 and 1900 cm^{-1} match nicely with major peaks in the H^+AlaAla spectrum; the smaller peak near 1450 cm^{-1}, and the apparent peak or shoulder near 1200 cm^{-1}, are also matched. The peak at 700 cm^{-1} for H^+AlaPhe (Fig. 2) is a characteristic phenyl-ring mode that appears in numerous spectra of Phe-containing ions. This feature would not be expected for H^+AlaAla, but the wavelength range of the presently available H^+AlaAla spectrum does not allow us to verify this prediction. Aside from this last possibility, there is no sign that the presence of the Phe side chain gives any significant spectroscopic characteristics compared with the Ala side chain in this wavelength range. There is an apparent small blue shift of the peaks near 1150 and 1790 cm^{-1} in H^+AlaPhe, which has no obvious relation to any perturbation by the Phe side chain. The smaller features in the present spectrum near 1100, 1300 and 1600 are probably too weak to be discerned in the H^+AlaAla spectrum, but in any case, according to the assignments based on the calculated TransA1 configuration, none of these features correspond to modes that are distinctively related to the Phe side chain. Furthermore, in contrast to the obvious appearance of cation–pi interactions in the calculated structures of metal–ion complexes of aromatic amino acid-containing molecules, the structures calculated for conformations of the protonated dipeptides show no indication of specific interactions of the proton with the aromatic ring. Thus the present work does not point toward any interesting effects attributable to the presence or absence of the aromatic side chain in the protonated dipeptides.

There is a notable contrast between protonated and metalated AlaPhe [10]. In the case of metalation (Na^+ and K^+) the metal ion participates in a strong cation–pi interaction with the phenyl ring, which plays a central role in structuring the conformation of the

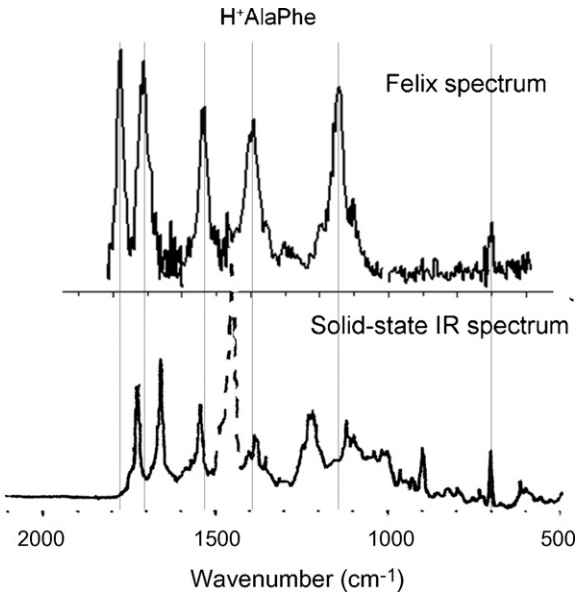

Fig. 5. Comparison of the gas-phase IRMPD spectrum of H^+AlaPhe with the spectrum of HClAlaPhe in a liquid-crystal matrix (Ref. [9]), both at room temperature. The intense feature near 1470 cm^{-1} in the matrix spectrum shown here with a broken curve is a matrix interference.

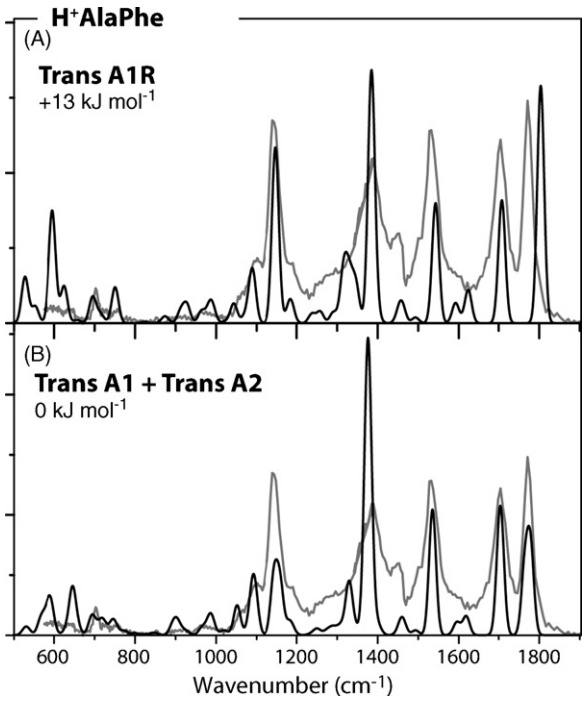

Fig. 6. Comparison of the experimental spectrum of H^+AlaPhe (gray) to (A) the calculated spectrum of TransA1R (which is the favorable conformation of $H^+AlaPheCl^-\cdot 2H_2O$, as determined by X-ray crystallography), and (B) an overlay of equally weighted spectra of the two most stable gas-phase conformations, TransA1 and TransA2. Note that the differences are pronounced for the pair of peaks between 1700 and 1800 cm^{-1}.

ionic complex. However, in the case of protonation, there is no apparently important interaction of the proton with the phenyl ring. The conformation is governed by hydrogen bonding interactions involving the Lewis-basic atoms, and the orientation of the phenyl side chain is largely unconstrained in its position relative to the charge site.

4. Comparison with the solid matrix spectrum reported for HClAlaPhe

One of the goals of the present study was to compare the gas-phase spectrum with the recently published solid matrix IR spectrum of H^+AlaPhe·Cl [9]. The spectra are compared in Fig. 5. At first sight the correlation is poor, showing little resemblance. One major discrepancy is the large peak in the matrix spectrum near 1470 cm^{-1} which has no counterpart in the gas-phase spectrum. Comparison with other spectra reported in the same solid matrix [19] indicates that this is a matrix absorption band. Accordingly, this region of the spectrum is plotted with a dashed line in Fig. 5. Even ignoring this feature, there are significant discrepancies between both spectra, and we suggest that the condensed-phase spectrum actually corresponds primarily to an H-bonded cyclic dimer form of the carboxylic acid group: several features correspond well to expected features in typical (neutral) carboxylic acid dimers, but poorly to features of the vapor-phase spectra that are normally assigned to the monomers of the acids. Three features of the spectrum suggest the dimer: (1) for the monomer the C=O stretch of the carboxyl group is expected at 1750–1780 cm^{-1} in the gas phase [20], and somewhat lower, ~1760 cm^{-1}, in condensed-phase. However, it shifts down closer to 1700 for the condensed-phase dimer [21,22] (near 1710 cm^{-1} in the gas phase [20]), in agreement with the highest-energy peak (1715 cm^{-1}) in the matrix spectrum shown here. (2) The strong peak at ~1220 cm^{-1} in the matrix spectrum is in a region where no condensed-phase monomer carboxylic acid or amide peak is expected, no strong peak is predicted from the calculations for this molecule, and no strong peak is observed in gas-phase amino acids, protonated amino acids, protonated dialanine or the present protonated AlaPhe spectrum. However, this is a reasonable place for a C–O stretching mode of a carboxylic acid dimer (1218 cm^{-1} in formic acid [21]). (3) The strong peak at 900 cm^{-1} in the matrix spectrum is in a region characteristic of the out-of-plane OH bend of carboxylic acid dimers (~930 cm^{-1}) [21–23], but does not correspond to any expected strong peak of the monomer. It is also fully expected that the molecule would form the cyclic dimer as its principal condensed-phase form [22], which is the normal situation for molecules with free carboxyl groups. This means that the comparison of gas-phase and condensed-phase spectra in Fig. 5 is not a direct comparison, but is rather a comparison of the protonated monomer (gas phase) versus the protonated dimer (condensed phase).

The amide II band (N–H bend) appears near 1530 cm^{-1} in both spectra. The amide I band (amide C=O stretch) at 1705 cm^{-1} (gas) is red-shifted to 1660 cm^{-1} (solid).

4.1. The crystal-state structure of $H^+AlaPheCl^-\cdot 2H_2O$ in comparison with the gas-phase cation structure

As noted above, the X-ray structure [8] of the H^+AlaPhe moiety of the $H^+AlaPheCl^-\cdot 2H_2O$ crystal clearly showed the TransA1R structure, in contrast to the TransA1 and TransA2 structures that we assigned to the gas-phase ion. Our arguments for rejecting the TransA1R structure in the gas phase are both spectroscopic and computational. Spectroscopically, we focus on this specific question in Fig. 6, which compares the TransA1R conformation with an equal mixture of TransA1 and TransA2 conformations. It is seen that the only clear distinction is in the splitting of the two peaks in the 1720–1800 cm^{-1} region, which is predicted to be considerably smaller for TransA1 and TransA2 than TransA1R. (This splitting reflects the differential in the interaction of the amide H with the C=O group of the carboxyl (TransA1 and TransA2) versus the COH group (TransA1R), which affects the position of the 1750 cm^{-1} vibration (carboxyl C=O stretch) while having no effect on the 1720 cm^{-1} vibration (amide C=O).) The splitting predicted

for TransA1 and TransA2 is clearly in better agreement with the IRMPD spectrum than that predicted for TransA1R.

Considering this assignment computationally, Table 1 shows that TransA1 and TransA2 are preferred over TransA1R by about 10 kJ mol^{-1} (free energies), which is a significant difference for relative determinations of the stabilities of similar conformations by this computational approach. These conformations are expected to be interconvertible at room temperature, since only rotation around a single bond is needed, so equilibrium favoring the more stable TransA1 and TransA2 structures over TransA1R should be readily achieved in the ICR cell. This conformational switch between crystalline and gas-phase environments is understandable: In the crystal the position of the OH group is stabilized by a strong hydrogen bond to one of the water molecules of crystallization (Scheme 1), which is not present in the gas phase.

There is some confusion in Ref. [9] about their computational results. The structure shown in their Scheme 2, which is close to the X-ray crystal structure, is described as their minimized structure and is similar to TransA1′R. However, their Table 1 describes a different structure, apparently close to TransA2, which would be more likely to be their actual minimum-energy result (see our Table 1). Our results shown in Table 1 confirm that the carboxyl-rotated TransA1R family of structures, which includes the X-ray structure TransA1R, is significantly higher in energy than the most stable structures in gas phase.

4.2. Comparison with H$^+$AlaTyr and H$^+$TyrAla

In a recent related study, Stearns et al. [11] used a cryogenic 22-pole trap (~6 K) to trap and characterize the two protonated dipeptides H$^+$[Ala,Tyr]. Using ultraviolet (UV) photodissociation and UV/IR double resonance experiments, the population of conformers could be mapped, and the conformer-specific IR spectra in the H-stretching region could be observed. Using B3LYP and a scaling factor of 0.954, relative conformer energies were calculated for families of conformers, and excellent fits were obtained between the IR spectra of the assigned conformers and their corresponding calculated IR spectra.

Comparing our computational results with theirs confirms that the H$^+$[Ala,Phe] and H$^+$[Ala,Tyr] systems are very similar, with few thermochemical effects attributable to the tyrosine hydroxyl versus phenylalanine. Table 1 correlates the labeling of those conformers that were calculated in both studies. The relative energies are the same in all cases within better than 2 kJ mol^{-1}. H$^+$AlaPhe and H$^+$AlaTyr are both predicted to have several low-lying conformers within about 1 kJ mol^{-1} of the ground state, while both H$^+$PheAla and H$^+$TyrAla are predicted to have a unique ground state conformation lying about 4 kJ mol^{-1} below the next higher conformer. For H$^+$AlaTyr at 6 K their experimental results indicated only one conformer with observable abundance (Family I *anti*/*anti*, corresponding to our TransA1). Our room temperature results could not distinguish between the two nearly isoenergetic conformers TransA1 and TransA2, and any combination of these would fit our results, although the presence of both conformers can be weakly inferred from the fit to the peak near 1150 cm^{-1} (see Fig. 6). For H$^+$TyrAla their experiments indicated at least two conformers (not counting the syn/anti-distinction), assigned as Family I *anti* and *gauche*. This corresponds nicely to our room temperature result for H$^+$PheAla that the lowest energy TransA1 conformer fits the spectrum well, without ruling out admixtures of other higher-energy TransA type conformers on the basis of our spectrum. Thus these two studies are entirely compatible in their conclusions about the conformer preferences of these systems. Since the IR spectra from their study are in a different wavelength region from the present study, no direct spectroscopic comparisons are possible.

The results of Stearns et al. suggest that a degree of caution is needed in predicting conformer populations based on computational differences of a few kJ mol^{-1}: For H$^+$TyrAla their experimental results indicate multiple conformers, compared to a computational suggestion of a single uniquely favorable conformation; while for H$^+$AlaTyr, experiment indicates a single conformation, although the computations point to the possibility of multiple isoenergetic conformations.

4.3. Spectroscopy of the delocalized proton

There is an interesting conformational ambiguity in the B3LYP results for H$^+$AlaPhe. In the TransA1 conformation (calculated to be the most stable) the proton on NH_3^+ is hydrogen bonded to the amide C=O oxygen atom, but the proton can shift its position to give a local potential energy minimum forming a COH$^+$ moiety hydrogen bonded to NH_2; this structure is only 1 kJ mol^{-1} higher in energy (structure TransO1). Observationally, the IR peak near 1400 cm^{-1}, which is assigned to an H-bending mode related to this proton transfer, appears to be significantly broadened compared with other peaks in the spectra of both H$^+$AlaPhe (Fig. 2) and H$^+$PheAla (Fig. 3). Based on the calculated energetics, either of these two conformers could be populated, or both, or the actual conformation could involve an intermediate proton position or a shared proton sharing both sites. The calculated barrier to transfer the proton is 8 kJ mol^{-1}, whereas the zero-point energy for the hydrogen-stretching mode (fundamental at 2700 cm^{-1}) that corresponds to the proton transfer is 16 kJ mol^{-1}. Thus, it is quite possible to conceive of this as a shared or delocalized proton, or a distributed or "strong" hydrogen bond [24]. The presence of a broadened vibrational peak has often been associated with an ion conformation containing a delocalized proton, and both theoretical and observational aspects of such hydrogen bonding situations have been extensively studied in both gas phase [25–32] and condensed phases [33].

The predicted spectra for these two conformations are significantly different (Fig. 2, compare TransA1 and TransO1). Notably, structure TransO1 is predicted to have little intensity at the characteristic frequency of the NH_3^+ group slightly below 1400 cm^{-1}. If this were a simple situation with one of these conformations dominating, it should thus be easy to identify spectroscopically whether the proton is located predominantly near the nitrogen or near the oxygen, and indeed the observed spectrum indicates a predominant nitrogen-bound character for this proton in H$^+$AlaPhe (see Fig. 2). In view of the interest of this conformation, the relative energies of TransA1 and TransO1 were also compared with a DFT/MPW1PW91 calculation, which indicated a difference in favor of TransA1 of less than 1 kJ mol^{-1}. Thus these two functionals agree in showing a double-well potential energy surface with a difference in energy of the two wells equal to zero within computational uncertainty, and a barrier less than the zero-point energy. It is suggested that a spectroscopic signature of this "strong" hydrogen bond is an exceptionally broadened and strong IR peak near 1400 cm^{-1}.

The possibility of the proton occupying this delocalized region of the potential energy surface exists for several common situations that have been studied in gas-phase systems, including the following: (1) polypeptides protonated at the alpha nitrogen of the N-terminus with a hydrogen bond to the amide carbonyl oxygen, as in the present work; (2) protonated monomeric amino acid derivatives which protonate the alpha nitrogen at the N-terminus with a hydrogen bond to the carbonyl oxygen [34]; (3) cationized amino acids in a zwitterionic conformation where the NH_3^+ group is hydrogen bonded to one of the carboxylate oxygens [14,35,36]; (4) proton-bound dimer ions, which have been studied extensively [25–32]. With regard to situation (4), in their study of the symmetrical dimethyl-ether proton-bound complex, Li et al. [29]

concluded that the peak broadening in the IRMPD spectrum could be accounted for by conformational sampling effects.

Possible examples of situation (3) are seen in spectra of some amino acids cationized with Cs^+, Rb^+ and perhaps K^+. Examples are tryptophan [14], serine [35] and threonine [36], all of which show a strong, broad peak at about 1400 cm^{-1} attributed to the COH hydrogen which has the hydrogen bond to the NH_2 group (and can thus undergo the internal proton transfer to the NH_3^+ zwitterionic conformation). It is believed that the COH configuration is the ground state in all of these cases, but the NH_3^+ zwitterion configuration is probably accessible, resulting in the type of double potential energy well that we are considering. Armentrout et al. [35] consider that for Cs^+Serine a fraction of the complexes actually has this hydrogen transferred to give the zwitterion configuration. Rodgers et al. [36], considering serine and threonine, discuss the nature of the modes in terms of interconversion of the proton between the CS and ZW configurations. This proton sits in a double well closely analogous to the proton under consideration in H^+AlaPhe, and we can speculate that the appearance of a broad H-bending peak in all of these spectra reflects a similar delocalized-proton situation. The postulated broadening of the 1400 cm^{-1} feature in ions characterized by situation (1), which we suggest here, is a variation of the delocalized-proton spectroscopy that deserves further study. A similar situation in protonated AlaAla has been given a convincing analysis based on Car-Parrinello dynamics simulation [3], which should offer a powerful approach for the present case as well.

5. Conclusions

IRMPD spectra have been recorded for the protonated dipeptides AlaPhe and PheAla and compared to DFT calculated spectra. Resulting low-energy structures have been compared to those determined by matrix isolation infrared spectroscopy and by X-ray crystallography, and for H^+AlaAla and H^+[Ala,Tyr] by IR spectroscopy. Both the spectroscopy and the computed thermochemistry indicate that the gas-phase structure of H^+AlaPhe differs from the crystal structure with respect to the orientation of the COOH group. Evidently, hydrogen bonding of the hydroxyl hydrogen to one of the water molecules of crystallization stabilizes the less-favored COOH orientation when the cation is embedded in the crystal lattice. It is notable that comparison of X-ray and IRMPD data is able to uncover this subtle conformational switch.

Comparison with the gas-phase spectrum of H^+AlaAla indicates that the presence of the aromatic Phe residue has little effect on the spectroscopy or the conformation of the peptide backbone, other than introducing additional phenyl-ring features around 700 cm^{-1}. This is in contrast with metalated cations, where cation–pi interaction between the ring and the metal ion has profound effects on the conformation and spectroscopy. Also, no major spectroscopic or structural differences were found upon reversing the sequence of the residues.

A good comparison between the present spectrum of H^+AlaPhe spectrum and that of the same ion in a solid matrix environment was unfortunately not possible. Although it was possible to correlate some features attributed to the amide modes, the prominent vibrational modes of the C-terminus did not correlate well, and we concluded that the matrix spectrum is most likely that of the dimerized form of the protonated peptide.

Correlation with the low-temperature study of the similar H^+AlaTyr and H^+TyrAla systems in the 22-pole rf trap showed behavior of the corresponding dipeptides that was the same within the scope of the possible comparisons.

It is suggested that the peak near 1400 cm^{-1} is broadened in the present spectra, as well as in various other gas-phase spectra of similar ions protonated on NH_2 with H-bonding to carbonyl. These protonated dipeptides should provide an interesting set of cases for study of the H-stretch/bend interaction and the mode anharmonicities in this delocalized-proton geometry.

Acknowledgments

RCD acknowledges support from the National Science Foundation, grant PIRE-0730072, and expresses gratitude for generous support by FOM during an extended visit. This work is part of the research program of FOM, which is financially supported by the "Nederlandse Organisatie voor Wetenschappelijk Onderzoek" (NWO). The skillful assistance by the FELIX staff is gratefully acknowledged. Construction and shipping of the instrument was made possible with funding from the National High Field FT-ICR Facility (grant #CHE-9909502) at the National High Magnetic Field Laboratory, Tallahassee, FL. We thank Professors John R. Eyler and Alan G. Marshall for their collaboration with the FT-ICR project.

Appendix A. Supplementary data

Supplementary data associated with this article can be found, in the online version, at doi:10.1016/j.ijms.2009.02.001.

References

[1] B. Lucas, G. Gregoire, J. Lemaire, P. Maître, J.M. Ortega, A. Rupenyan, B. Reimann, J.P. Schermann, C. Desfrancois, Phys. Chem. Chem. Phys. 6 (2004) 2659.
[2] H.-B. Oh, C. Lin, H.Y. Hwang, H. Zhai, K. Breuker, V. Zabrouskov, B.K. Carpenter, F.W. McLafferty, J. Am. Chem. Soc. 127 (2005) 4076.
[3] G. Gregoire, M.P. Gaigeot, D.C. Marinica, J. Lemaire, J.P. Schermann, C. Desfrancois, Phys. Chem. Chem. Phys. 9 (2007) 3082.
[4] N.C. Polfer, J. Oomens, S. Suhai, B. Paizs, J. Am. Chem. Soc. 127 (2005) 17154.
[5] N.C. Polfer, J. Oomens, S. Suhai, B. Paizs, J. Am. Chem. Soc. 129 (2007) 5887.
[6] N.C. Polfer, B. Paizs, L.C. Snoek, I. Compagnon, S. Suhai, G. Meijer, G. von Helden, J. Oomens, J. Am. Chem. Soc. 127 (2005) 8571.
[7] J.A. Stearns, O.V. Boyarkin, T.R. Rizzo, J. Am. Chem. Soc. 129 (2007) 13820.
[8] M. Cortrait, Y. Barrans, Acta Cryst. B30 (1974) 1018.
[9] B.B. Koleva, T. Kolev, S.Y. Zareva, M. Spiteller, J. Mol. Struct. 831 (2007) 165.
[10] N.C. Polfer, J. Oomens, R.C. Dunbar, Chem. Phys. Chem. 9 (2008) 579.
[11] J.A. Stearns, M. Guidi, O.V. Boyarkin, T.R. Rizzo, J. Chem. Phys. 127 (2007) 154322.
[12] J. Valle, J.R. Eyler, J. Oomens, D.T. Moore, A.F.G. van der Meer, G. von Helden, G. Meijer, C.L. Hendrickson, A.G. Marshall, G.T. Blakney, Rev. Sci. Instrum. 76 (2005) 023103.
[13] N.C. Polfer, J. Oomens, Phys. Chem. Chem. Phys. 9 (2007) 3804.
[14] N.C. Polfer, J. Oomens, R.C. Dunbar, Phys. Chem. Chem. Phys. 8 (2006) 2744.
[15] B. Paisz, I.P. Csonka, G. Lendvay, S. Suhai, Rapid Commun. Mass Spectrom. 15 (2001) 637.
[16] R. Linder, M. Nispel, T. Haeber, K. Kleinermanns, Chem. Phys. Lett. 409 (2005) 260.
[17] W. Chin, I. Compagnon, J.-P. Dognon, C. Canuel, F. Piuzzi, I. Dimicoli, G. von Helden, G. Meijer, M. Mons, J. Am. Chem. Soc. 127 (2005) 1388.
[18] Y. Inokuchi, Y. Kobayashi, T. Ito, T. Ebata, J. Phys. Chem. A 111 (2007) 3209.
[19] B. Jordanov, B. Schrader, J. Mol. Struct. 347 (1995) 389.
[20] J.M. Bakker, L. MacAleese, G. von Helden, G. Meijer, J. Chem. Phys. 119 (2003) 11180.
[21] I. Wolfs, H.O. Desseyn, J. Mol. Struct. (Theochem.) 360 (1996) 81.
[22] I. Wolfs, H.O. Desseyn, Appl. Spectrosc. 50 (1996) 1000.
[23] E.S. de la Blanca, J.L. Nunez, P. Martinez, An. Quim. Ser. A 82 (1986) 480.
[24] C.L. Perrin, J.B. Nielson, Ann. Rev. Phys. Chem. 48 (1997) 511.
[25] D.T. Moore, J. Oomens, A.F.G. van der Meer, G. von Helden, G. Meijer, J. Valle, A.G. Marshall, J.R. Eyler, Chem. Phys. Chem. 5 (2004) 740.
[26] T.D. Fridgen, L. MacAleese, P. Maître, T.B. McMahon, P. Boissel, M. Lemaire, Phys. Chem. Chem. Phys. 7 (2005) 2747.
[27] T.D. Fridgen, T.B. McMahon, L. MacAleese, J. Lemaire, P. Maître, J. Phys. Chem. A 108 (2004) 9008.
[28] K.R. Asmis, N.L. Pivonka, G. Santambrogio, M. Brummer, C. Kaposta, D.M. Neumark, L. Woster, Science (2003) 1375.
[29] X. Li, D.T. Moore, S.S. Iyengar, J. Chem. Phys. 128 (2008) 184308.
[30] J.R. Roscioli, L.R. McCunn, M.A. Johnson, Science 316 (2007) 249.
[31] K. Rajabi, T.D. Fridgen, J. Phys. Chem. A 112 (2008) 23.
[32] R. Wu, T.B. McMahon, J. Am. Chem. Soc. 129 (2007) 4864.
[33] P. Gilli, V. Bertolasi, L. Pretto, V. Ferretti, G. Gilli, J. Am. Chem. Soc. 126 (2004) 3845.
[34] A. Simon, L. MacAleese, P. Maître, J. Lemaire, T.B. McMahon, J. Am. Chem. Soc. 129 (2007) 2829.
[35] P.B. Armentrout, M.T. Rodgers, J. Oomens, J.D. Steill, J. Phys. Chem. A 112 (2008) 2248.
[36] M.T. Rodgers, P.B. Armentrout, J. Oomens, J.D. Steill, J. Phys. Chem. A 112 (2008) 2258.